P1.5 MEASUREMENTS OF HUMIDITY IN THE ATMOSPHERE: VALIDATION EXPERIMENTS (MOHAVE) OVERVIEW OF THE CAMPAIGN AND FIRST RESULTS

T. Leblanc[1]*, I. S. McDermid[1], J. Howe[1], R. Aspey[1], T. D. Walsh[1], H. Vömel[2], T. G. McGee[3], L. Twigg[3], G. Sumnicht[3], D. Whiteman[3], B. Demoz[3], R. Connell[4], D. Venable[4], R. Forno[5], M. Cadirola[6], G. McIntire[7], and L. Miloshevic[8].

[1] Jet Propulsion Laboratory, California Institute of Technology, Wrightwood, CA. USA
[2] University of Colorado, CIRES, Boulder, CO. USA
[3] NASA Goddard Space Flight Center, Greenbelt, MD. USA
[4] Howard University, Washington, D.C. USA
[5] Universidad de San Andres, La Paz. Bolivia
[6] Ecotronics Venture, Clarksburg, MD. USA
[7] SGT, Lanham, MD. USA
[8] National Center for Atmospheric Research, Boulder, CO. USA

1. INTRODUCTION

Water vapor has long been identified as a key constituent of the atmosphere and, for example, it has a major role in the radiative balance of the upper troposphere and lower stratosphere. Over the past decade, a long-term increase in the lower stratospheric water vapor has been detected, the cause of which is not fully understood. Due to its very low concentration near and above the tropopause and because of its very high spatial and temporal variability in the troposphere, measuring water vapor and understanding and quantifying accurately its role on climate remains a challenging exercise. In order to contribute to this understanding as well as to support the validation of satellite measurements, the Network for the Detection of Atmospheric Composition Change (NDACC, formerly known as NDSC), has recently considered including the water vapor measurements using Raman lidar in its suite of long-term measurements. A high capability water vapor Raman lidar was therefore built at the Jet Propulsion Laboratory (JPL) Table Mountain Facility in California (34.4ºN, elev. 2285-m), with the overall objective of measuring water vapor in the upper troposphere/lower stratosphere (UT/LS) with an accuracy equal to, or better than 5% (Leblanc et al., manuscript in preparation). The new lidar began routine operation in spring 2005 and the first major validation campaign, called "Measurements of Humidity in the Atmosphere: Validation Experiments" (MOHAVE), took place in October 2006. MOHAVE involved several remote sensing and in-situ techniques and was very successful with more than 40 balloon launches and over 240 hours of lidar measurements. An overview of the campaign operations and achievements is described in this paper.

2. INSTRUMENTS DEPLOYMENT

2.1 *Lidars*

In addition to the JPL-TMF water vapor Raman lidar (referred to as "JPL lidar" hereafter), two other lidars were brought to TMF from NASA Goddard Space Flight Center (GSFC), Greenbelt, MD to participate to the campaign. The "Aerosol and Temperature" lidar (referred to as "AT lidar" hereafter) measures aerosol backscatter ratio, temperature and tropospheric water vapor, and has been used as a comparison standard in many past NDACC inter-comparison campaigns (McGee et al., manuscript in preparation). The Scanning Raman Lidar (referred to as "SRL lidar" hereafter) measures water vapor, aerosol and cloud properties, and has also participated in many field campaigns (Whiteman et al., 2006). All three lidars (JPL, AT, and SRL) utilize the same technique, i.e., calculating the ratio of the Raman-backscattered signals returned respectively at 387 nm by atmospheric nitrogen, and 407.5 nm by atmospheric water vapor. A detailed description of this technique is given for example in (Sherlock et al., 1999). There are two limitations with this technique: 1) the instrument loses sensitivity as we approach the tropopause due to the decreasing of water vapor concentration and 2) the instrument needs careful calibration, often requiring an external source of information, for example a water vapor measurement from radiosonde. One of the primary goals of MOHAVE was to evaluate the performance of the lidars near the tropopause. The JPL instrument routinely has acquired data up to 16-20 km but the measurements at such high altitudes could never be validated due to the lack of correlative measurements having the required accuracy. Such validation at high altitudes was finally possible during MOHAVE thanks to the use of balloon borne in-situ sensors of appropriate accuracy.

2.2 *In-situ balloon measurements*

A crucial component of MOHAVE was the comparison of the lidar measurements to the in-situ balloon borne measurements from the Cryogenic Frost-point Hygrometer (CFH). The water vapor measurement by the CFH is described in details in (Vömel et al., 2006). The CFH is presently considered as one of the most reliable instruments to measure water vapor in the UT/LS. The CFH water vapor profiles are therefore considered as our reference in all the upcoming MOHAVE investigations. A total of ten CFH were launched between October 19 and 28.

Vaisala RS92 radiosondes were also widely used during MOHAVE. Their performance has been

* *Corresponding author address:* Dr. Thierry Leblanc, JPL – Table Mountain Facility, 24490 Table Mountain Rd, Wrightwood, CA 92397-0367; email: leblanc@tmf.jpl.nasa.gov

described for example in [Miloshevich et al., 2006]. The RS92 water vapor measurements are not as accurate as those of the CFH and have significant biases (for example, a dry bias at low temperatures, and/or low relative humidity, i.e., in the upper troposphere). Two types of RS92 were used during MOHAVE. A total of forty-one RS92K provided by JPL and eight RS92 with GPS capability provided by GSFC were launched during the campaign. In order to study the repeatability of the RS92 measurements, eleven balloon payloads included two RS92. Overall, nine payloads contained one CFH and two RS92, one payload contained one CFH and one RS92, and two payloads contained two RS92. The rest of the payloads each contained a single RS92K.

2.3 *Other instruments*

In addition to the three lidars, the CFH and RS92 mentioned above, two GPS receivers (one located at TMF and operated by JPL (Manucci, Personal Communication), and another brought by the SRL/GSFC staff for the campaign) produced integrated water vapor data. A microwave instrument based at TMF and operated in the framework of NDACC by the Naval Research Laboratory (Nedoluha et al., 1995) routinely produces water vapor profiles above 30 km. An experimental, non-validated, water vapor total column product was provided for MOHAVE. The GPS and microwave data can be used to help calibrate the water vapor Raman lidars. However none of the work involving these datasets is presented or discussed here. To complement the already large set of instruments and techniques, the JPL tropospheric ozone lidar was run simultaneously with the water vapor lidars during the entire the campaign and one ECC ozonesonde was launched simultaneously with each CFH. Though very valuable scientifically, these measurements are of minor interest to the water vapor validation exercise described here.

2. SUMMARY OF OPERATIONS

As already mentioned, one primary goal of the campaign was to evaluate the performance of the water vapor Raman lidars in the UT/LS, a region where signal-to-noise ratio is very low. Since the water vapor lidar measurement is background-noise limited, highest priority was given to five nights centered on the new moon, i.e., October 19-23, 2006. Additional priority was given to nights with best Aura satellite overpass, i.e., October 14 and October 28. The mobile SRL and AT lidar trailers arrived at TMF on October 8. The SRL instrument suffered major damage during transportation, and the entire system had to be reconfigured to be operational for the campaign. As a result, the largest telescope of the system could not be used and only the 20-cm-diameter telescope was used during the campaign. It obviously affected the quality of the SRL measurements with usable water vapor profiles only below 10-12 km. The damage to SRL was the only glitch in the campaign operations. The first high-priority night (Friday the 13th) was cloudy for half of the time but the next fifteen nights remained entirely clear. At least one or two RS92 were launched each night between October 14 and October 28 (more than two launches per night were often performed). On October 28, the data from four consecutive RS92K flights were received simultaneously with the JPL and GSFC Vaisala ground systems, which allowed evaluation of the same sonde measurements using two different Vaisala software versions. The first CFH was launched on October 19. From that night on, one CFH per night was launched. Two CFH were launched on October 21. Each payload including a CFH also included an ozonesonde and two RS92. The CFH launch times were optimized to coincide with the best Aura-MLS overpass. Most nights, the AT and JPL lidars were operated all night long. However it was agreed between the MOHAVE participants to analyze the lidar signals over shorter time windows to better match the in-situ measurement times. The standard analyzing procedure was to provide a 1-hour-integrated lidar profile starting at the time of each launch, and 1-h-integrated profile starting one hour after launch. Additional integration windows were chosen to provide nightly-integrated profiles (profiles reaching higher altitudes) and to provide short-integration profiles (to study short-term variability within the same night).

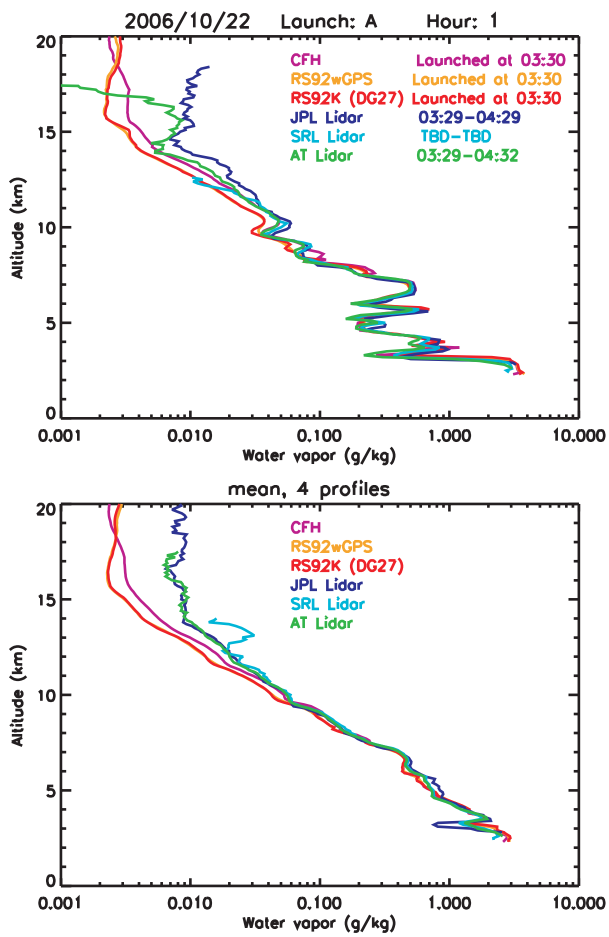

Figure 1. *Top: Example of a water vapor profile measured simultaneously by all three lidars, the CFH, and two RS92 sondes. Bottom: Average of the four available profiles measured simultaneously by all these instruments*

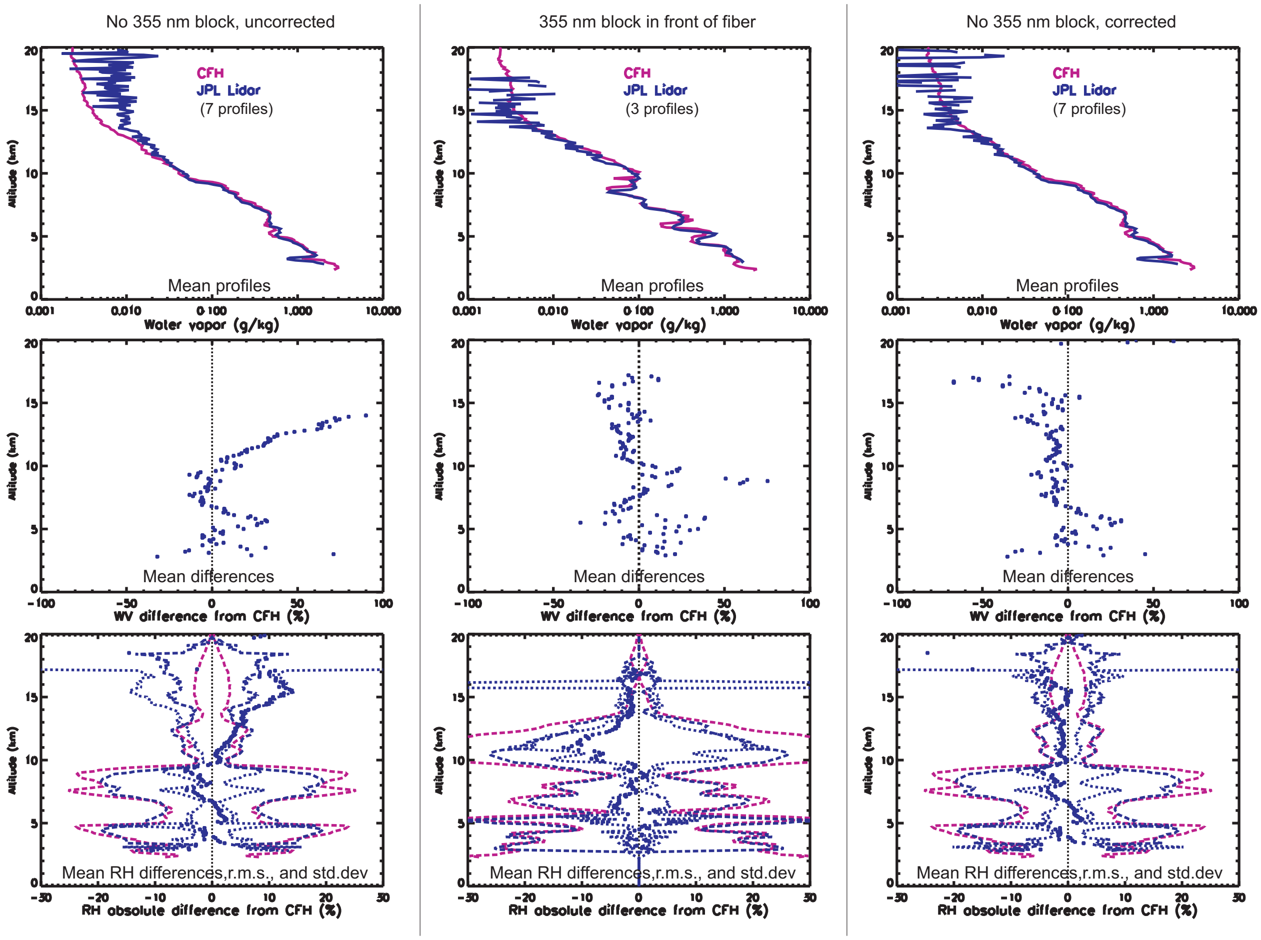

***Figure 2**. Comparison of the JPL lidar mean water vapor profiles with the CFH in three different configurations. Left: All available measurements with no blocking filter and no empirical correction; Middle: All available measurements with a blocking filter in front of the fiber optics; Right: No blocking filter, but empirical correction is applied in the retrieval. See text for details.*

The various combinations of balloon launch and lidar running times allowed investigation of the following topics: 1) All instruments compared to each other; 2) Lidar to CFH comparisons; 3) Lidar to Lidar; 4) RS92 to CFH; 5) RS92 to RS92 (repeatability); 6) water vapor variability in the troposphere and in the UTLS; 7) Lidar calibration issues. Preliminary results for each of these topics are now briefly reviewed.

3. RESULTS

3.1 Comparisons between all instruments

Figure 1 (top) shows an example of one-hour water vapor profiles measured simultaneously by all three lidars, and the corresponding simultaneous CFH and (two) RS92 profiles. Figure 1 (bottom) shows the average of all available profiles measured simultaneously by all instruments (which includes only the profiles measured during the time all lidar instruments ran in their standard configuration).

There are two main conclusions from figure 1: 1) all instruments capture the fine water vapor vertical structures below 10 km very well, and 2) all lidars show a systematic wet bias, and the RS92 a systematic dry bias, in the upper troposphere when compared to the CFH. The Vaisala radiosondes dry bias has been observed and investigated before but it is the first demonstration for the lidars of a significant wet bias increasing from the lower to the upper troposphere.

3.2 Lidars and CFH: Lessons learned

MOHAVE provided the first opportunity to investigate the performance of the water vapor Raman lidar in the upper troposphere. After making various experimental tests, the wet bias observed in figure 1 was found to be the result of parasitic fluorescence in the lidars' water vapor channels. All three lidars revealed the presence of fluorescence because all three systems are pushed to their limit of detection and therefore become very sensitive to predictable residual fluorescence in the instrument optics. In the case of the JPL lidar, the fluorescence was identified in the fiber optic connecting the large telescope to the receiver box. Figure 2 illustrates the impact of this fluorescence and how it can be removed or corrected. The three figures on the left side show results obtained with the initial lidar configuration and with no correction to the water vapor retrieval. The three figures in the middle show results obtained after a 355 nm blocking filter was installed at the entrance of the fiber optic. The wet bias observed on the left figures is absent in the middle figures.

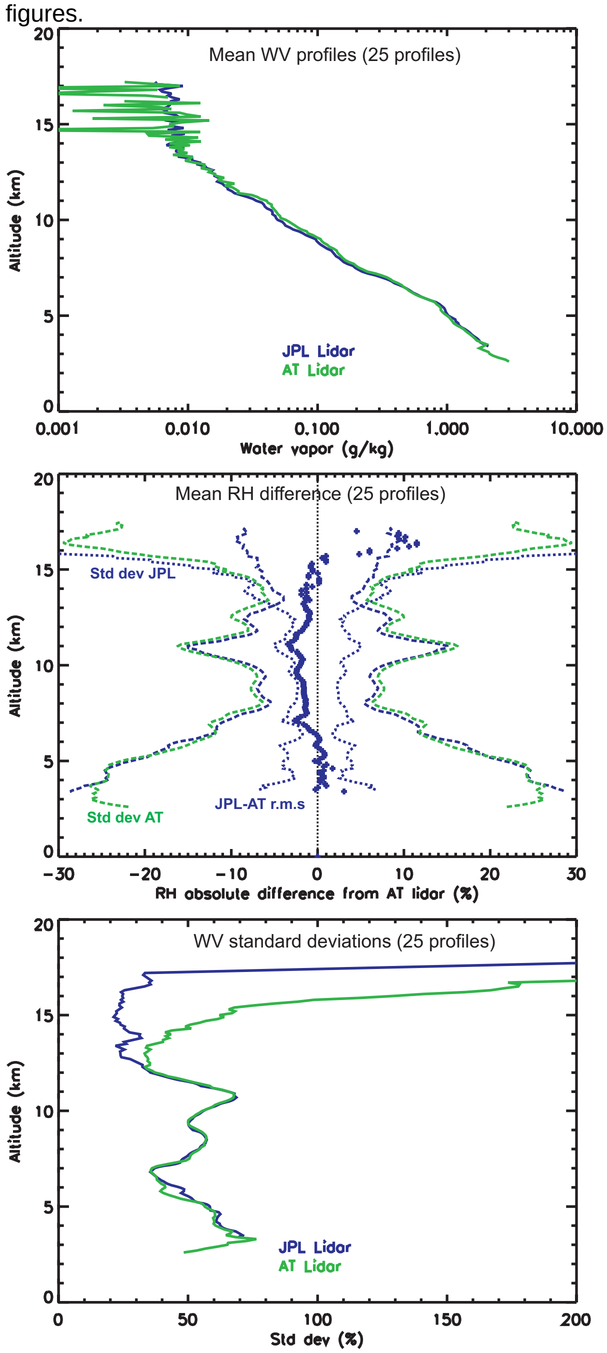

Figure 3. *Average of all water vapor profiles simultaneously measured by the AT and JPL lidars.*

The lidar data contaminated by fluorescence can be corrected empirically. The fluorescence signal is excited by the very intense Rayleigh lidar return at 355 nm. It is a spectrally wide signal having the same spatio-temporal characteristics as that of the Rayleigh signal itself. In other words, the signal leaking into the 407 nm channels is directly proportional to the 355 nm signal received in a separate channel assuming that this channel has receiving properties similar to that of the 407 nm channels. The three figures on the right hand side of figure 2 show water vapor retrieved from the exact same measurements as that of the figures on the left hand side but after an empirical correction was applied in the retrieval. In this example the fluorescence was removed by subtracting 1/750th of the 387-nm medium-intensity signal from the 407-nm high intensity signal. The advantage of this technique is that it allows the correction of all the measurements made by the JPL water vapor lidar since it started operating in 2005. One drawback is that the fraction of Rayleigh signal to be subtracted is somewhat arbitrary and in this case, solely based on the comparisons with the CFH measurements.

Note that in the case of the JPL lidar, there is no 355-nm Rayleigh channel with receiving properties similar to that of the 407-nm channel to be corrected. We therefore used the Nitrogen (387-nm) backscatter signal instead of the Rayleigh signal. The only difference between the two signals is the possible presence of particular-scattering-induced fluorescence that would not be accounted for when using the Raman 387-nm signal. However, several experimental tests made on the SRL system showed no aerosol contribution whatsoever, and the correction made on the SRL results ended up to be equivalent whether using the Rayleigh or Raman signal.

3.3 Lidar to lidar:

Figure 3 shows the comparison of the mean water vapor profiles obtained from all profiles simultaneously measured by the AT and JPL lidars. Very consistent individual profiles, mean, and standard deviations were obtained, leading to less than a few percent relative humidity differences between the two instruments. A small negative systematic bias is observed and can be explained by the different calibration technique used for each instrument. For the AT lidar a single constant is used while for the JPL lidar the best fit to the simultaneous CFH or RS92 profile in the lower troposphere is used.

3.4 RS92 to CFH:

Figure 4 shows the comparison of the mean relative humidity (RH) profiles obtained from all profiles simultaneously measured by the CFH and the RS92 radiosondes. Eight of the ten CFH payloads also included two RS92 radiosondes. The radiosonde data from each type of sonde were transmitted to two separate Vaisala ground-systems, referred to as "DG27" and "wGPS" hereafter. The Vaisala DIGICORA v2.7 is used by JPL to receive data from the JPL RS92K sondes, and the DIGICORA v3.5 is used by the GSFC lidar staff to receive data from the GSFC RS92 sondes equipped with GPS. The datasets referred to as "RS92K DG35" correspond to data received from R92K sondes on the JPL ground system, then re-processed by DG35 using the "Re-flight Simulation" capability of the GSFC software. This way the various versions of the Vaisala

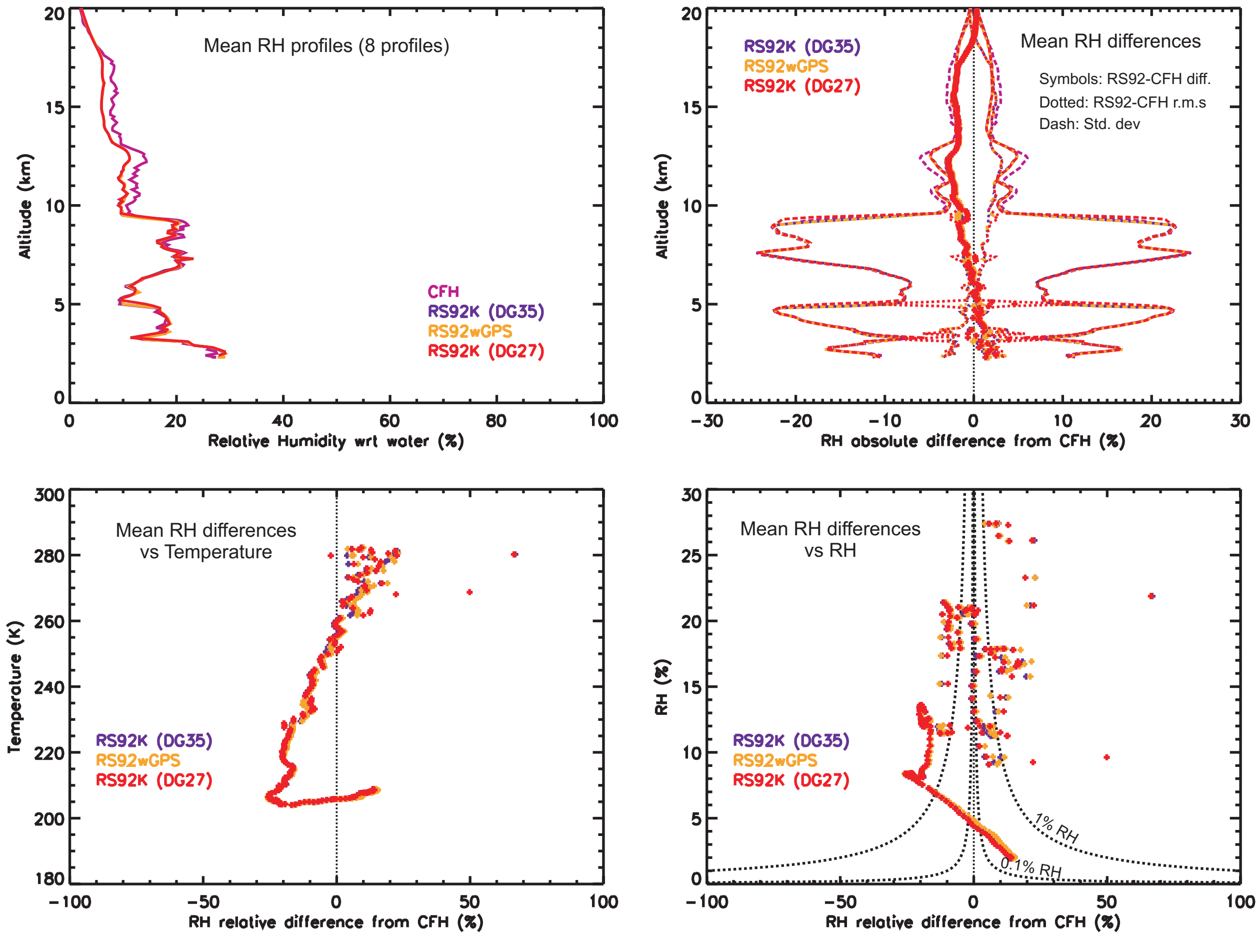

Figure 4. *Top-left: Mean relative humidity profiles simultaneously measured by the CFH and RS92 when two RS92 sondes were attached to the payload (see text for differences between the RS92 datasets). Top-right and bottom: Mean RH differences*

software could be cross-validated. The main feature on figure 4 is the systematic dry bias of the RS92 compared to the CFH. This bias has been observed before and various empirical corrections (time-lag, temperature, solar radiation, etc.) have been developed in the past. These corrections are expected to be applied to the MOHAVE profiles in future investigations.

3.5 RS92 to RS92: Measurement repeatability

Figure 5 shows the comparison of the mean RH profiles obtained from all the profiles measured when a pair of RS92 radiosondes was attached to the balloon payload. The observed differences between the two radiosondes are mainly caused by small differences in the data smoothing and editing procedure of the Vaisala software. There is no apparent systematic bias except at low temperature and low relative humidity when the observed bias reaches 0.2% RH.

On the last night of the campaign (October 28), the data from single radiosondes launched on four balloons were received simultaneously by both the JPL DIGICORA v2.7 and the GSFC DIGICORA v3.5 ground stations. The mean results from each software version are shown in figure 6. A very small systematic bias of 0.2% RH was observed between the two versions. The biases observed on figures 5 and 6 are currently being investigated.

3.6 Short-term water vapor variability

Figure 7 shows a “curtain plot” of RH produced by the GSFC AT lidar acquisition software. This 2D time-altitude cross-section illustrates the high variability at short time scales that often characterizes tropospheric water vapor. On this particular night, a RS92 radiosonde was launched at around 03:30 UT coinciding with the short dry episode near 5 km altitude that can be seen on figure 7. As a result, the lidar 1-h or 2-h integrated measurements yields a much wetter atmosphere at this altitude than the radiosonde. This illustrates the difficulty to sometimes adequately interpret differences between measurements obtained from different platforms and reveals potential difficulties in calibrating the lidar measurements by using a correlative measurement such as the radiosonde.

3.7 Raman lidar calibration issues

In order to detect long-term trends in the lower stratosphere, the calibration procedure should be considered very carefully, and made as stable as possible with time. One method consists of launching a radiosonde every time the lidar is running and use the radiosonde profile to best "fit" the lidar profile in a given altitude range, and deduce the corresponding calibration constant. If both radiosonde and lidar measurements are perfect, simultaneous, and co-located, the same calibration constant should be found each time. In reality this calibration constant varies by about 5%.

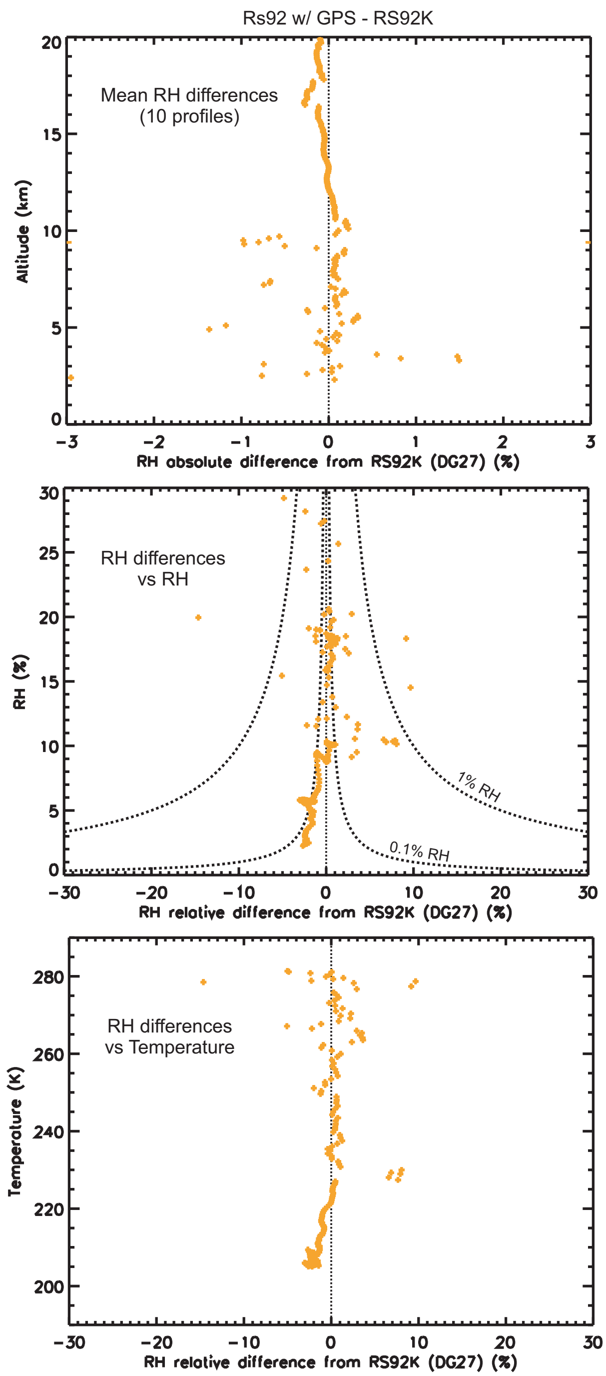

Figure 5. *Mean differences of all RH profiles simultaneously measured by all RS92 radiosonde pairs*

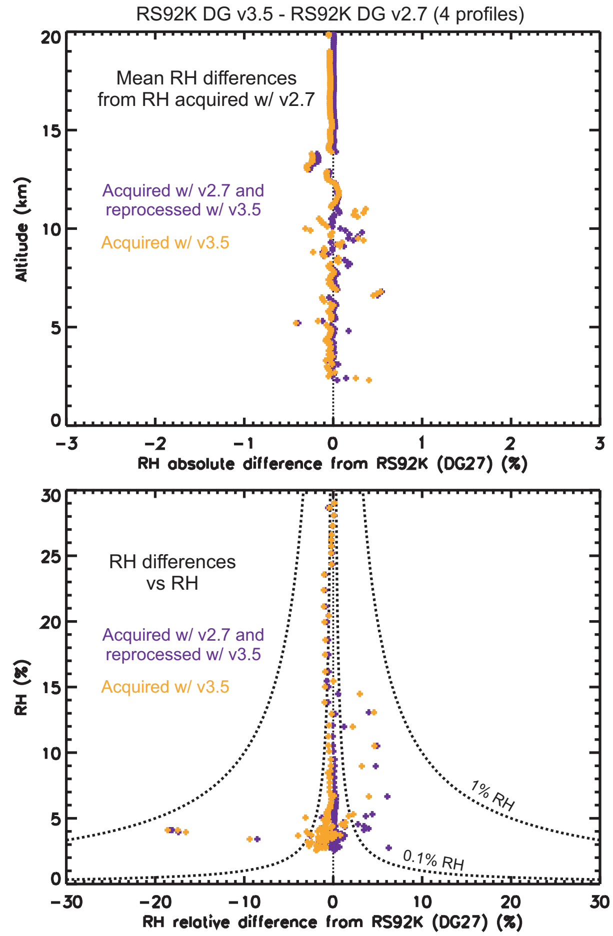

Figure 6. *Mean differences of the four RH profiles obtained from single RS92K sondes and simultaneously received by both the JPL and GSFC Vaisala ground-systems*

During the entire MOHAVE campaign, the AT lidar water vapor retrieval used a single calibration constant determined from previous campaigns while the JPL water vapor retrieval used a calibration constant calculated for each profile from the best matching radiosonde or CFH profile available at the time. To assess the possible impact of the calibration method on the accuracy of the measurement, the JPL water vapor profiles were compared to those of the AT lidar for two retrieval configurations: 1) the normal JPL retrieval, i.e., using a different calibration constant for each profile, and 2) a modified retrieval that normalizes the JPL measurements to the AT measurements, which is equivalent to using a single calibration constant throughout the campaign. For all the profiles measured simultaneously by the JPL and AT lidars the standard deviation of the JPL lidar measurements in each retrieval configuration is compared to that of the AT lidar. The results are shown in Figure 8. When the JPL lidar measurement is calibrated to the AT lidar measurement, the two standard deviations match perfectly up to 12-13 km altitude where statistical noise starts to contaminate the measurements. In the other hand, when each JPL measurement is normalized to each simultaneous radiosonde measurement, the standard deviation increases by 5% near 10 km altitude. This additional variability was introduced by the fact that even simultaneous and co-located radiosonde profiles do not always match the longer-time -integrated lidar profiles. This result illustrates the upcoming challenges of finding the appropriate calibration method to be able to detect small long-term trends in water vapor.

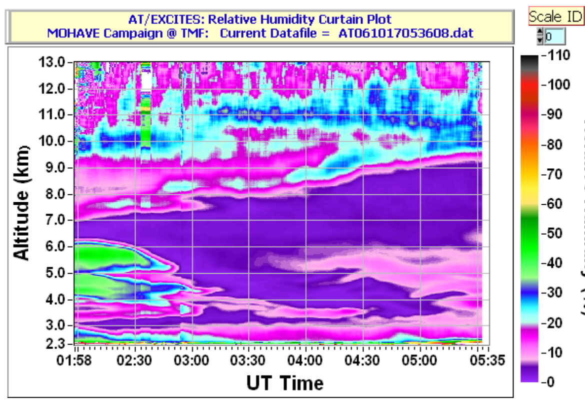

Figure 7. *Four-hour "curtain-plot" of relative humidity measured by the AT lidar on October 17, 2006*

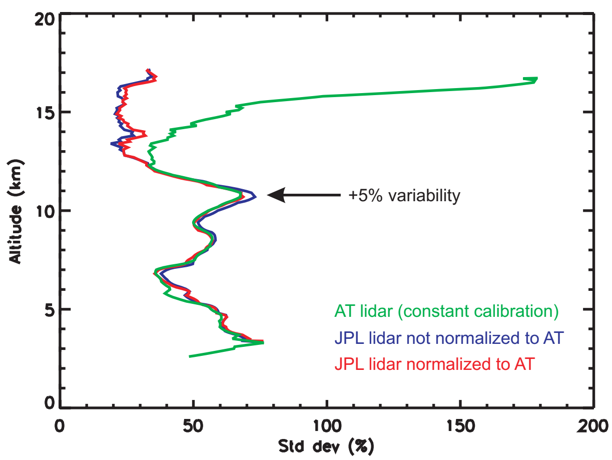

Figure 8. *Comparison of standard deviations calculated from water vapor profiles calibrated with two different methods. See text for details*

4. CONCLUSION

The MOHAVE campaign was held at the JPL Table Mountain Facility, California from October 14 to 28, 2006. The main objective of the campaign was to evaluate the performance of the water vapor Raman lidar in the UT/LS. Using more than 240 hours of lidar measurements, and more than 50 in-situ CFH and RS92 profiles, various biases were clearly observed between the different measuring techniques: When taking the CFH measurement as the reference, a wet bias, negligible in the lower and mid-troposphere then increasing in the upper troposphere, was systematically observed on the measurements of all three participating lidars. A dry bias was observed on the RS92 measurements in the upper troposphere (where temperature and relative humidity values are very low). This dry bias has been observed in previous campaigns, and various corrections to the measurements have been applied in the past. These corrections will be refined in the future using the MOHAVE results.

The lidar wet bias was found to be caused by fluorescence in all three lidars' receiving systems. The measurement of very low water vapor mixing ratios near the tropopause requires the lidar to be pushed to its detection limit, thus making it very sensitive to this type of well known residual aberration of the optical components. After the presence of fluorescence was demonstrated, it was decided in the case of the JPL lidar to re-configure the receiver in order to permanently redirect the intense 355-nm returned signal (the source of contamination) out of the fiber optics used ahead of the water vapor detectors. Similar technical modifications are planned for the SRL and AT lidars.

Due to the short time elapsed since the end of the campaign, many topics have not been yet investigated. However, it is clear that the wealth of information obtained during the campaign will permit many new findings in the future.

REFERENCES

Miloshevich, L. M., H. Voemel, D. N. Whiteman, B. M. Lesht, F. J. Schmidlin, and F. Russo, 2006: Absolute accuracy of water vapor measurements from six operational radiosonde types launched during AWEX-G, and implications for AIRS validation. *J. Geophys. Res.*, **111**, D09S10, doi:10.1029/2005JD006083

Nedoluha, G. E., R. M. Bevilacqua, R. M. Gomez, D. L. Thacker, W. B. Waltman, and T. A. Pauls, 1995: Ground-based measurements of water vapor in the middle atmosphere, *J. Geophys. Res.*, **100**, 2927-2939.

Sherlock, V., A. Garnier, A. Hauchecorne, and P. Keckhut, 1999: Implementation and validation of a Raman lidar measurement of middle and upper tropospheric water vapor, *J. Appl. Optics.*, **38**, 5838-5850.

Vömel, H., D. David, and K. Smith, 2006: Accuracy of tropospheric and stratospheric water vapor measurements by the Cryogenic Frost point Hygrometer (CFH): Instrumental details and observations, *J. Geophys. Res.*, in press.

Whiteman, D. N., et al., 2006: Raman Water Vapor Lidar Measurements During the International H2O Project. I. Instrumentation and Analysis Techniques, *J. Atmos. Oceanic Technol.*, **23**, 157-169.